

# On the Origin of Traveling Pulses in Bistable Systems

C. Elphick

*Centro de Física No Lineal y Sistemas Complejos de Santiago, Casilla 17122, Santiago, Chile*

A. Hagberg\*

*Center for Nonlinear Studies and T-7, Theoretical Division, Los Alamos National Laboratory, Los Alamos, NM 87545*

B. A. Malomed†

*Department of Interdisciplinary Studies, Faculty of Engineering, Tel Aviv University, Ramat Aviv 69978, Israel*

E. Meron‡

*The Jacob Blaustein Institute for Desert Research and the Physics Department, Ben-Gurion University, Sede Boker Campus 84990, Israel*

(November 18, 2018)

The interaction between a pair of Bloch fronts forming a traveling domain in a bistable medium is studied. A parameter range beyond the nonequilibrium Ising-Bloch bifurcation is found where traveling domains collapse. Only beyond a second threshold the repulsive front interactions become strong enough to balance attractive interactions and asymmetries in front speeds, and form stable traveling pulses. The analysis is carried out for the forced complex Ginzburg-Landau equation. Similar qualitative behavior is found in the bistable FitzHugh-Nagumo model.

PACS number(s):

Traveling waves far from equilibrium are often formed when a uniform state is destabilized by a Hopf bifurcation occurring at a finite wavenumber [1]. Traveling waves or pulses also form from parity breaking bifurcations of stationary patterns [2]. A related mechanism that has not received adequate attention involves a parity breaking *front bifurcation* in which a stationary front solution loses stability to a pair of counter-propagating front solutions [3–6]. This bifurcation, sometimes referred to as the nonequilibrium Ising-Bloch (NIB) bifurcation, has been found in chemical reactions [7,8] and in liquid crystals [9,10]. Bistable systems, which do not necessarily support stationary patterns, may exhibit traveling pulses and waves beyond the NIB bifurcation. Activator-inhibitor systems with non-diffusing inhibitors provide a good example. For fast inhibitor kinetics initial domain patterns always coarse grain and converge to a uniform state. For sufficiently slow kinetics, and beyond the NIB bifurcation, traveling pulses, periodic wavetrains, and spiral waves appear.

Numerical studies of systems with a NIB bifurcation indicate that traveling pulses do not appear immediately at the front bifurcation point. Instead, there is an intermediate parameter range where initial domains may travel but eventually collapse. Only past a second threshold parameter value do initial domains converge to stable traveling pulses [5]. In this paper we study the interactions between a pair of traveling fronts in this intermediate parameter range. We find that the balance of repulsive front interactions with attractive interactions and an asymmetry between leading and trailing fronts gives this threshold parameter value.

We choose to study the parametrically forced complex Ginzburg-Landau (CGL) equation

$$A_t = (\mu + i\nu)A + (1 + ic_1)A_{xx} - (1 + ic_3)|A|^2A + \gamma A^* + \alpha, \quad (1)$$

where  $A(x, t)$  is a complex field and  $\nu, c_1, c_3$  and  $\gamma$  are real parameters. The parameter  $\alpha$  can be a complex number, but since the final results we present here do not depend on its imaginary part we assume  $\alpha$  is also real [11]. The CGL equation ( $\gamma = \alpha = 0$ ) is often obtained as an envelope equation for an extended system undergoing a Hopf bifurcation at zero wavenumber [12]. Then, the variable  $A(x, t)$  describes weak modulations of the homogeneous oscillations. The terms  $\alpha$  and  $\gamma A^*$  in (1) represent, respectively, the effect of parametric forcing with equal and twice the system's natural oscillation frequency [13,14]. Equation (1) has been introduced recently in the context of liquid crystals [15].

The parametric forcing term  $\gamma A^*$  breaks the phase shift symmetry,  $A \rightarrow Ae^{i\phi}$ , of Eqn. (1) and reduces the one-parameter family of cw solutions of the CGL equation,  $A = A_0 e^{i(\nu - c_3\mu)t + i\phi}$ ,  $0 < \phi < 2\pi$ , to two pairs of stable-unstable solutions with fixed  $\phi$  values, arising in saddle-node bifurcations. Equation (1) therefore describes a bistable extended system of two stable uniform states that oscillate with different phases. The second forcing term,  $\alpha$ , breaks the parity symmetry ( $A \rightarrow -A$ ) of these two states. The front solutions we will be concerned with connect these two states at  $x \rightarrow \pm\infty$ .

A simpler, gradient version of Eqn. (1) is obtained by omitting the linear and nonlinear dispersion terms:

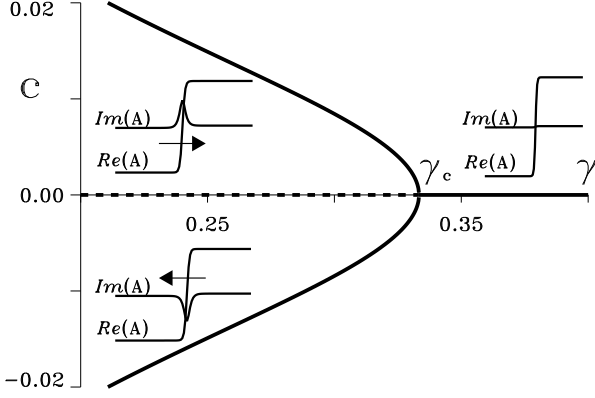


FIG. 1. The nonequilibrium Ising-Bloch (NIB) bifurcation for front solutions of Eqn. (1). For  $\gamma > \gamma_c$  there is a single stable Ising front with zero speed (solid line). For  $\gamma < \gamma_c$  the Ising front is unstable (dashed line) and a pair of stable counterpropagating Bloch fronts appears (solid lines). Parameters:  $\mu = 1.0$ ,  $\nu = 0.01$ ,  $c_1 = c_3 = \alpha = 0.0$ .

$$A_t = \mu A + A_{xx} - |A|^2 A + \gamma A^* + \alpha. \quad (2)$$

A physical application of (2) is Rayleigh-Bénard convection with periodic spatial modulation of the cell height [16] or heating [17]. When  $\alpha = 0$ , Eqn. (2) has three types of stationary front solutions

$$I(x; \sigma) = \sigma A_0 \tanh\left(\frac{1}{\sqrt{2}} A_0 x\right), \quad (3)$$

$$B_{\pm}(x; \sigma) = \sigma A_0 \tanh(kx) \pm i\sqrt{\mu - 3\gamma} \operatorname{sech}(kx), \quad (4)$$

where  $A_0 = \sqrt{\mu + \gamma}$ ,  $k = \sqrt{2\gamma}$  and  $\sigma = \pm 1$  is the front polarity which stems from the reflection symmetry  $x \rightarrow -x$  of Eqns. (2) and (1). The front solutions  $I(x; \sigma)$  and  $B_{\pm}(x; \sigma)$  are equivalent to Néel (Ising) and Bloch domain walls in ferromagnets with weak anisotropy [4] and will be referred to as Ising and Bloch fronts. The Ising front  $I(x; \sigma)$  loses stability as  $\gamma$  is decreased past the critical value  $\gamma_c = \mu/3$ . At that point the two Bloch fronts  $B_{\pm}(x; \sigma)$  appear and are stable [4].

The non-gradient terms associated with  $\nu$ ,  $c_1$  and  $c_3$  remove the degeneracy of the three stationary solutions (3) and (4). With any of these terms nonzero, the two Bloch fronts propagate in opposite directions at a speed proportional to the corresponding coefficient,  $\nu$ ,  $c_1$  or  $c_3$  [4]. In that case, a plot of the front velocity,  $c$ , versus  $\gamma$  yields the NIB bifurcation diagram shown in Fig. 1.

To study front interactions we consider the symmetric ( $\alpha = 0$ ) and nearly gradient case, where front solutions of (1) can be expanded around front solutions of the gradient system (2). We introduce a small parameter  $\epsilon \ll 1$  and assume that the constants  $\nu$ ,  $\alpha$ ,  $c_1$ , and  $c_3$  are all of order  $\epsilon$ . We also assume proximity to the Ising-Bloch bifurcation point,  $\mu - 3\gamma \sim \sqrt{\epsilon}$ . A traveling domain solution of Eqn. (1) is sought as

$$A(x, t) = B_+[x - x_l(T); +1] + B_-[x - x_r(T); -1] - A_0 + R(x, T), \quad (5)$$

where  $x_r$  and  $x_l$  are the positions of the leading (right) and trailing (left) Bloch fronts,  $T = \epsilon t$  is a slow time,  $B_{\pm}$  are given by (4), and  $R$  is a small correction term of order  $\epsilon$ . The two polarities ( $\sigma = \pm 1$ ) are necessary to construct a domain bounded by the fronts. The two types of Bloch fronts,  $B_-$  and  $B_+$ , make the domain *traveling* instead of shrinking or expanding. We assume that the domain is much wider than the width of the fronts,  $k^{-1}$ , or more accurately, that  $\exp[-2k(x_r - x_l)] \sim \epsilon \ll 1$ .

Our objective is to derive equations of motion for the front positions,  $x_l$  and  $x_r$ . Using the ansatz (5) in (1) and following the method of Refs. [18], we find the following solvability condition for the right (leading) front:

$$\begin{aligned} \dot{x}_r \int_{-\infty}^{\infty} \left| \frac{\partial B_-}{\partial x} \right|^2 dx + \alpha \int_{-\infty}^{\infty} \frac{\partial B_-^*}{\partial x} dx \\ + i\nu \int_{-\infty}^{\infty} \frac{\partial B_-^*}{\partial x} B_- dx + ic_1 \int_{-\infty}^{\infty} \frac{\partial B_-^*}{\partial x} \frac{\partial^2 B_-}{\partial x^2} dx \\ - ic_3 \int_{-\infty}^{\infty} \frac{\partial B_-^*}{\partial x} |B_-|^2 B_- dx + \int_{-\infty}^{\infty} \frac{\partial B_-^*}{\partial x} \mathcal{N} dx \\ + c.c. = 0, \end{aligned} \quad (6)$$

where *c.c.* stands for the complex conjugate. A similar condition is obtained for the left (trailing) front. In Eqn. (6) the dot over  $x_r$  represents the derivative with respect to the fast time  $t$ , and  $\mathcal{N}$  is a nonlinear interaction term

$$\begin{aligned} \mathcal{N} = (B_-^* + B_+^*)(A_0 - B_+)(B_- - A_0) \\ + (B_- + B_+)(A_0 - B_+)(B_-^* - A_0) \\ + (B_- + B_+)(A_0 - B_+^*)(B_- - A_0), \end{aligned}$$

where the arguments of  $B_{\pm}$  are as in (5). Analytical evaluation of the nonlinear interaction integral in (6) leads to the following equations, with  $\eta = \sqrt{\mu - 3\gamma}$  [18]:

$$\begin{aligned} \frac{4}{3} k A_0 \dot{x}_r = 2\alpha + \pi\eta[-\nu + c_3\mu + (c_1 - c_3)\gamma] \\ - 8A_0^3 e^{-2k(x_r - x_l)} + 4A_0\eta^2 e^{-k(x_r - x_l)}, \\ \frac{4}{3} k A_0 \dot{x}_l = -2\alpha + \pi\eta[-\nu + c_3\mu + (c_1 - c_3)\gamma] \\ + 8A_0^3 e^{-2k(x_r - x_l)} - 4A_0\eta^2 e^{-k(x_r - x_l)}. \end{aligned} \quad (7)$$

Combining Eqns. (7) gives a single equation of motion for the distance between the two fronts,  $L = x_r - x_l$ :

$$k A_0 \dot{L} = 3\alpha - 12A_0^3 e^{-2kL} + 6A_0\eta^2 e^{-kL}. \quad (8)$$

The first term on the right hand side describes the effect of the broken symmetry between the two Bloch fronts; the initial domain expands (shrinks) in time when the leading front is faster (slower) than the trailing front. The second term describes an attractive front interaction

generated by the real parts of the Bloch front solutions. The last term, generated by the imaginary parts of the Bloch front solutions, describes a longer range repulsive interaction. The repulsive interaction strengthens as  $\gamma$  is decreased below the Ising-Bloch bifurcation point,  $\gamma_c = \mu/3$ , and becomes dominant at sufficiently small  $\gamma$  values.

Notice that in Eqn. (8) the non-gradient terms associated with  $\nu$ ,  $c_1$ , and  $c_3$  have disappeared. To leading order the effect of these terms is to grant the two Bloch fronts equal speeds. Therefore the distance between the fronts is not affected. This suggests that the existence and stability of pulse solutions (moving domains) of Eqn. (1) can be studied starting from the gradient version (2). The latter can be written as  $A_t = -\delta H/\delta A^*$ , where  $\delta/\delta A^*$  stands for the variational derivative, and the Lyapunov function (pseudo-Hamiltonian) is

$$H = \int_{-\infty}^{+\infty} \mathcal{H} dx, \quad (9)$$

$$\mathcal{H} = |A_x|^2 - \mu|A|^2 + \frac{1}{2}|A|^4 - \frac{1}{2}\gamma[A^2 + (A^*)^2] - \alpha(A + A^*).$$

This gradient representation implies relaxational dynamics toward a minimum of  $H$ . The part of  $H$  which depends upon the separation distance  $L$  between the Bloch fronts can be found following Ref. [19]. The resulting effective *pseudopotential* of the interaction for  $\mu \approx 3\gamma$  is

$$U(L) = \frac{4A_0^2}{3\sqrt{3}} \left( -4\sqrt{2}e^{-2kL} + \frac{2\sqrt{2}\eta^2}{k^2}e^{-kL} - \frac{\alpha}{k^2}L \right). \quad (10)$$

The extrema of  $U(L)$  coincide with stationary solutions of (8).

To find traveling pulse solutions of (1), which correspond to stationary (fixed point) solutions of (8), we set  $\dot{L} = 0$  in (8) or  $dU/dL = 0$  in (10) and solve the resulting quadratic equation for  $z = \exp(-kL)$ . The solutions are:

$$L = -k^{-1} \ln \left( \eta^2 \pm \sqrt{\eta^4 + 4A_0\alpha} \right) + 2k^{-1} \ln 2A_0. \quad (11)$$

In the symmetric case,  $\alpha = 0$ , and for  $\eta > 0$ , there is only one (finite) pulse solution. A linear stability analysis indicates the solution is unstable. This result complies with an earlier finding reported in Ref. [20]. For  $\alpha > 0$  the leading front is faster than the trailing front. Again, only one pulse solution exists and a linear stability analysis indicates the solution is unstable. The same conclusion follows from a graph of Eq. (10): the single pulse solution corresponds to a maximum of the interaction pseudopotential  $U(L)$ . For  $\alpha < 0$  no pulse solutions exist if  $\eta^4 < 4A_0|\alpha|$ . A saddle-node pair of pulse solutions appears at  $\gamma = \gamma_p(\alpha)$ , where  $\gamma_p(\alpha)$  solves  $(\mu - 3\gamma_p)^2 = 4\sqrt{\mu + \gamma_p}|\alpha|$ . Graphs of these solutions in

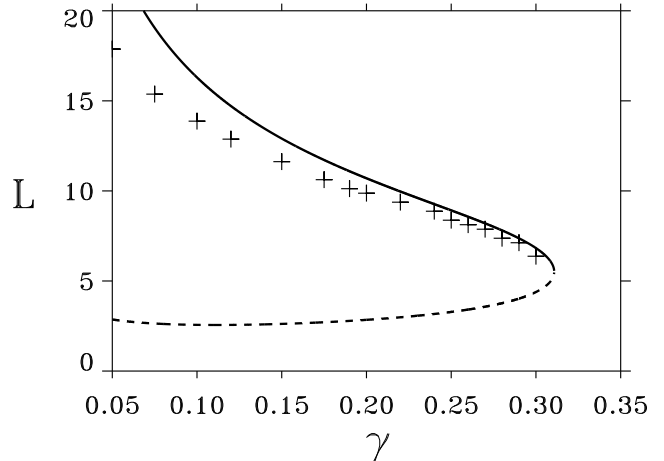


FIG. 2. The distance,  $L$ , between the front and back of a pulse solution for  $\gamma$  near the NIB bifurcation. The solid and dashed lines represent the stable and unstable branches solutions from Eqn. (11). The crosses are data from direct numerical solution of Eqn. (1). Parameters:  $\mu = 1$ ,  $\nu = 0.01$ ,  $\alpha = -0.001$ ,  $c_1 = c_3 = 0$ .

the  $L - \gamma$  plane are shown in Fig. 2. The upper and lower branches represent stable and unstable solutions, and pertain to a minimum and a maximum of  $U(L)$ , respectively. Also shown in Fig. 2 are results from direct numerical solutions of Eqn. (1) showing the stable branch. The agreement for small  $\eta$  is within 5%. The shape of the stable traveling pulse is shown in Fig. 3a.

The conclusion that no stable pulses exist for  $\alpha > 0$  is a result of the specific ansatz (5) for an “up” pulse as shown Fig. 3a. From the symmetry  $A \rightarrow -A$  of (1), a symmetric stable “down” pulse exists for  $\alpha > 0$ . The shape of this pulse is displayed in Fig. 3b. A phase diagram of all stable front and pulse solutions is shown in Fig. 4a. Three main regions can be distinguished: (I) The entire Ising regime,  $\gamma > \gamma_c = \mu/3$ , where only a stable Ising front solution exists. In this region domains shrink or expand but do not travel or form pulses. (II) A region in the Bloch regime,  $\gamma_p(\alpha) < \gamma < \gamma_c$ , where a pair of stable counterpropagating Bloch fronts exist. In this region domains travel but do not form pulses; they either expand to infinity or shrink and collapse. (III) The rest of the Bloch regime,  $\gamma < \gamma_p(\alpha)$ , excluding the  $\alpha = 0$  line (the  $\gamma$  axis), where stable traveling pulses exist in addition to the pair of Bloch fronts. The  $\gamma$  axis separates regions of up and down pulses.

This behavior is rather general. Shown in Fig. 4b is an analogous phase diagram for the bistable FitzHugh-Nagumo (FHN) model

$$\begin{aligned} u_t &= u - u^3 - v + u_{xx}, \\ v_t &= \epsilon(u - a_1v - a_0) + \delta v_{xx}, \end{aligned} \quad (12)$$

where  $u$  and  $v$  are real fields and  $\epsilon, \delta, a_1$  and  $a_0$  are real constants. The parameters  $\epsilon$  and  $a_0$  play a similar role

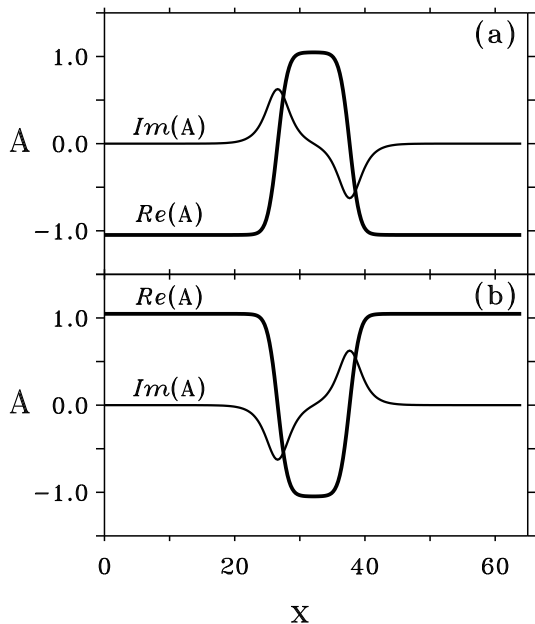


FIG. 3. Pulse solutions to Eqn. (1) near the NIB bifurcation. (a) A stable “up” pulse,  $\alpha < 0$ . (b) A stable “down” pulse  $\alpha > 0$ .

as  $\gamma$  and  $\alpha$ , respectively, and the same three regions (I), (II) and (III) appear in the  $\epsilon$ - $a_0$  plane.

The existence of an intermediate parameter region where traveling domains collapse rather than converge to stable pulses, has been observed in numerical simulations of model equations [5,21]. It is also expected to be observed in a number of experimental systems including catalytic reactions on platinum surfaces [21], liquid crystals subjected to rotating magnetic fields [9,10,22], oscillatory chemical reactions subjected to periodic forcing [23], and the Ferrocyanide-Iodate-Sulfite reaction [24].

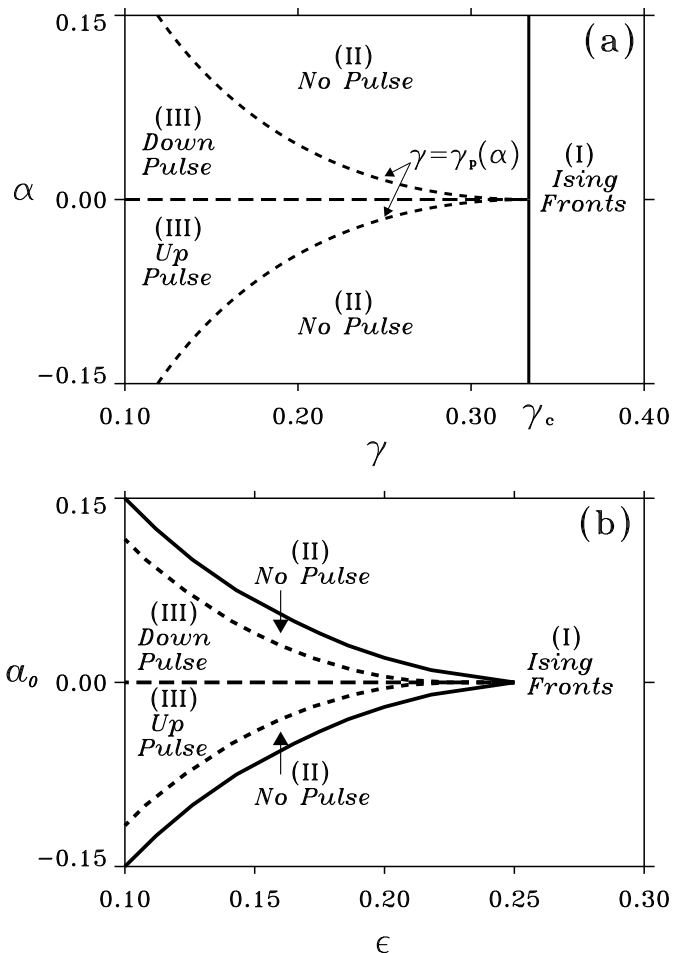


FIG. 4. (a) A phase diagram in the plane of the forcing parameters,  $\alpha - \gamma$ , showing the regions of stable front and pulse solutions to the forced CGL equation. For  $\gamma > \gamma_c$  only Ising fronts exist and there are no pulse solutions. For  $\gamma < \gamma_c$  a pair of stable Bloch fronts exist but they only form a stable traveling pulse solution when  $\gamma < \gamma_p$ . Parameters:  $\mu = 1.0$ ,  $\nu = 0.05$ ,  $c_1 = c_3 = 0$ . (b) The bistable FHN equation (12) shows the same type of phase diagram in the  $\epsilon - a_0$  parameter plane. Parameters:  $a_1 = 2.0$ ,  $\delta = 0$ .

- 
- [1] B. A. Malomed, Zs. Phys. B **55**, 241 (1984); M. C. Cross and P. C. Hohenberg, Rev. Mod. Phys. **65**, 851 (1993).
  - [2] J. Buckmaster, SIAM J. Appl. Math. **44**, 40 (1984); B. A. Malomed and M. I. Tribelsky, Physica D (1984); P. Couillet and G. Iooss, Phys. Rev. Lett. **64**, 866 (1990).
  - [3] H. Ikeda, M. Mimura, and Y. Nishiura, Nonl. Anal. TMA **13**, 507 (1989).
  - [4] P. Couillet, J. Lega, B. Houchmanzadeh, and J. Lajzerowicz, Phys. Rev. Lett. **65**, 1352 (1990).
  - [5] A. Hagberg and E. Meron, Nonlinearity **7**, 805 (1994).
  - [6] M. Bode, A. Reuter, R. Schmeling, and H.-G. Purwins, Phys Lett. A **185**, 70 (1994).
  - [7] G. Haas, M. Bär, I. G. Kevrekidis, P. B. Rasmussen, H. -H. Rotermund, and G.Ertl, Phys Rev. Lett. **75**, 3560

- (1995).
- [8] D. Haim, G. Li, Q. Ouyang, W. D. McCormick, H. L. Swinney, A. Hagberg, and E. Meron, *Phys. Rev. Lett.* **77**, 190 (1996).
  - [9] T. Frisch, S. Rica, P. Coulet, and J. M. Gilli, *Phys. Rev. Lett.* **72**, 1471 (1994).
  - [10] S. Nasuno, N. Yoshimo, and S. Kai, *Phys. Rev. E* **51**, 1598 (1995).
  - [11] The imaginary part of  $\alpha$  may contribute, however, to higher order corrections not considered here.
  - [12] Y. Kuramoto, *Chemical Oscillations, Waves and Turbulence* (Springer, Berlin, 1984).
  - [13] C. Elphick, G. Iooss and E. Tirapegui, *Phys. Lett. A* **120**, 459 (1987).
  - [14] Equation (1) is obtained assuming that the detuning  $\nu$  of the forcing at the system's natural frequency is exactly half the detuning of the forcing at twice the natural frequency.
  - [15] T. Frisch and J.M. Gilli, *J. Phys. II France* **5**, 561 (1995).
  - [16] R. E. Kelly and D. Pal, *J. Fluid Mech.* **86**, 433 (1978); G. Z. Gershuni, E. M. Zhukhovitsky, and A. A. Nepomnyashchy, *Stability of Convective Flows*, (Nauka, Moscow, 1989) (in Russian).
  - [17] M. Lowe and J. P. Gollub, *Phys. Rev. A* **31**, 3893 (1985); P. Coulet, *Phys. Rev. Lett.* **56**, 724 (1986); E. Curado and C. Elphick, *J. Phys. A: Math. and General* **20**, 1205 (1987); L. Gil, G. Balzer, P. Coulet, M. Dubois, and P. Bergé, *Phys. Rev. Lett.* **66**, 3249 (1991); J. K. Bhat-tacharjee, *Phys. Rev. A* **43**, 819 (1991).
  - [18] C. Elphick, E. Meron, and E. A. Spiegel, *Phys. Rev. Lett.* **61**, 496 (1988); *SIAM J. Appl. Math* **50**, 490 (1990).
  - [19] B. A. Malomed and A. A. Nepomnyashchy, *Europhys. Lett.* **27**, 649 (1994).
  - [20] L. Korzinov, M. I. Rabinovich, and L. S. Tsimring, *Phys. Rev. A* **46**, 7601 (1992).
  - [21] M. Eiswirth and G. Ertl, in: *Chemical Waves and Patterns* edited by R. Kapral and K. Showalter (Kluwer Academic Publishers, 1995).
  - [22] K. B. Migler and R. B. Meyer, *Physica D* **71**, 412 (1994).
  - [23] V. Petrov, private communication.
  - [24] K. J. Lee and H. L. Swinney, *Phys. Rev. E* **51**, 1899 (1995).